Journal of Nuclear Materials 381 (2008) 284–289

Contents lists available at ScienceDirect

Journal of Nuclear Materials

journal homepage: www.elsevier.com/locate/jnucmat

Synthesis of rare earth phosphates in molten LiCl–KCl eutectic: Application to preliminary treatment of chlorinated waste streams containing fission products

Damien Hudry [a,d], Isabelle Bardez [a], Aydar Rakhmatullin [b,c], Catherine Bessada [b,c], Florence Bart [a], Stéphane Jobic [d], Philippe Deniard [d,*]

[a] CEA Marcoule DTCD/SECM/LDMC, BP 17171, 30207 Bagnols sur Cèze cedex, France
[b] Conditions Extrêmes et Matériaux Hautes Températures et Irradiations, CEMHTI-CNRS, 45071 Orléans cedex 2, France
[c] Université d'Orléans, Faculté des Sciences, BP 6749, 45067 Orléans cedex 2, France
[d] Institut des Matériaux Jean Rouxel, Université de Nantes, CNRS, 2 rue de la Houssinière, BP 32229, 44322 Nantes cedex 3, France

ARTICLE INFO

Article history:
Received 29 May 2008
Accepted 1 September 2008

ABSTRACT

The precipitation of rare earth phosphates (RE = La, Ce, Pr, Nd, and Lu), from $RECl_3$ was investigated in molten LiCl–KCl eutectic at 500 °C in air. Ammonium dihydrogenphosphate ($NH_4H_2PO_4$) was used as the phosphorus precursor. X-ray diffraction analysis indicated the formation of compounds with monazite (La, Ce, Pr, and Nd) or xenotime (Lu) structures. ^{31}P NMR spectroscopy measurements confirmed that lanthanum formed pure monazite, which indicates a $LaCl_3 \rightarrow LaPO_4$ conversion factor near 100%. These results demonstrate that the stoichiometric addition of $NH_4H_2PO_4$ is sufficient to obtain quantitative precipitation at 500 °C of anhydrous rare earth phosphates in molten LiCl–KCl. The use of this type of precursor, which has the advantage of not modifying the chemical composition of the medium after recovery of the rare earth phosphates, could be considered during the first step of purification of chlorinated baths containing fission products arising from spent fuel reprocessing by a pyrochemical process.

1. Introduction

Many countries are involved in the development of future ‘fourth-generation’ nuclear systems. Six reactor concepts were selected by the Generation IV International Forum (GIF) [1] to meet five fundamental criteria including economic competitiveness, enhanced safety, proliferation-resistant facilities, conservation of natural resources, and minimal waste production. To meet the last criterion, most (five out of six) of the systems selected should involve a closed fuel cycle with the objective of recovering all the actinides (U, Pu and the minor actinides). In this context, pyrochemical separation processes are currently being investigated as potential candidates for spent fuel reprocessing. The efforts of the International Scientific Community focus mainly on electrolytic methods (electrolysis and electrorefining) or reductive liquid–liquid extraction [2]. All these techniques are based on the use of non-aqueous solvents (inorganic salts and/or liquid metals) at high temperature.

Electrochemical separation in molten chloride media is one of the main non-aqueous processes used for spent fuel reprocessing. The main electrolysis step is carried out in an inorganic molten salt. The chloride media LiCl–KCl eutectic is very often used as the solvent because of its low melting point (353 °C). The actinides and fission products (FP) should be separated during this step. This method is expected to generate a variety of flows material (Fig. 1). The first (item 1, Fig. 1) consists of reusable material intended for fuel refabrication. The second flow (item 2, Fig. 1) comprises metallic elements that were not dissolved in the melt during separation of the actinides from the fission products. The final flow (item 3, Fig. 1) consists of the solvent in which should be dissolved FP chlorides ($FPCl_x$) representing three broad chemical families: alkalis (A), alkaline earths (AE) and rare earths (RE).

The accumulation of FP in the solvent will modify its physical and chemical properties. When the $FPCl_x$ concentration exceeds about 10 wt% in the melt it must generally be purified or regenerated to avoid affecting the actinide/FP separation efficiency. The hypothetical composition of a salt bath to be purified is shown Table 1 and Fig. 2.

Two alternatives are now being examined to manage the high-level waste constituted by the spent salt. The first considers the entire salt flow as an ultimate wasteform. However, this flow is chemically highly reactive and entirely water-soluble, and must therefore be conditioned in a chemical form that is compatible with long-term disposal, i.e., resistant to leaching and self-irradiation. Current Vitrification (an industrial process implemented for nitric acid solutions from the PUREX process) is poorly suited for this purpose because of poor chlorine loading in the glass network (<1.5 wt% for alkali silicate glass) [3]. Tests in the United States at the Argonne National Laboratory demonstrated the possibility of

---

[*] Corresponding author. Fax: +33 2 40 37 39 95.
E-mail address: philippe.deniard@cnrs-imn.fr (P. Deniard).

0022-3115/$ - see front matter © 2008 Elsevier B.V. All rights reserved.
doi:10.1016/j.jnucmat.2008.09.005

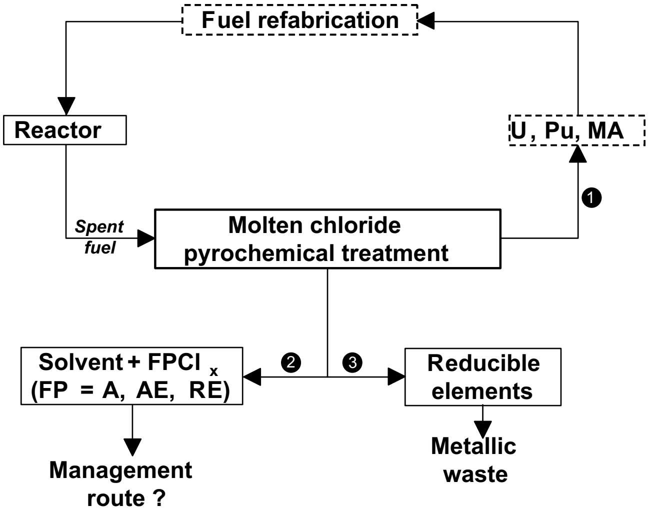

Fig. 1. Schematic representation of material flows likely to be generated by a pyrochemical process using molten chlorides to reprocess spent fuel (FP; fission product, A; actinide, AE; alkaline earth, RE; rare earth and MA; minor actinide).

Table 1
Hypothetical composition of a salt bath containing fission product chlorides; distribution by elements

Chlorides	wt%	Chlorides	wt%
LiCl	40	$PrCl_3$	0.757
KCl	50	$NdCl_3$	2.702
RbCl	0.194	$PmCl_3$	0.046
CsCl	1.301	$SmCl_3$	0.528
$SrCl_2$	0.587	$EuCl_3$	0.086
$BaCl_2$	0.923	$GdCl_3$	0.049
YCl_3	0.394	$TbCl_3$	0.001
$LaCl_3$	0.829	$DyCl_3$	0.001
$CeCl_3$	1.602		

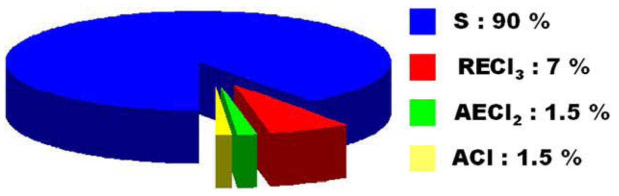

Fig. 2. Hypothetical composition of a salt bath containing fission product chlorides: distribution by families of elements. Percentage values are weight percentages (S; salt, RE; rare earth, AE; alkaline earth and A; alkaline).

conditioning the entire waste stream by the formation of a glass/sodalite composite [4], but this management strategy suffers from a major drawback concerning the final waste volume for disposal. Furthermore, using of chloroapatite ($Ca_5(PO_4)_3Cl$) or spodiosite (Ca_2PO_4Cl) are also being investigated for complete immobilization [5].

Considering that both the solvent and chlorine are inactive, the second management strategy is based on preliminary treatment of the flow so that only the fission products require conditioning. The main advantage compared with complete immobilization is the possibility of recycling the solvent, which is a key feature from both an economic and an environmental standpoint.

Concerning anhydrous preliminary treatment of chlorinated waste streams containing FP, most studies have addressed selective extraction of the REE. Cho et al. [6,7], for example, showed that rare earth chlorides (RE = La, Ce, Nd and Gd) can be converted to oxychlorides (REOCl, where RE = La, Nd and Gd) or oxide (CeO_2) simply by sparging oxygen through the molten LiCl–KCl eutectic. The $RECl_3 \rightarrow REOCl$ conversion factors vary with the temperature and sparging time, ranging from 94% (La) to 99.9% (Nd, Gd) at a temperature of 750 °C for a total sparging time of 7 h. The authors then verified that the conversion of oxychlorides to oxides (RE_2O_3; RE = La, Nd, and Gd) was possible by calcining in oxygen between 850 and 1200 °C depending on the type of rare earth element.

Other authors investigated the formation of rare earth phosphates with the generic formula $REPO_4$. These compounds crystallize as monazite or xenotime depending on the size of the cation [8]. They are generally synthesized by solid-state reactions at high-temperature (1100–1300 °C) [9]. When implemented with aqueous phases (sol–gel or precipitation) these methods generally yield hydrated phases requiring high-temperature calcining to obtain anhydrous phases. However, the use of molten chloride media considerably diminishes the temperature of formation of rare earth phosphates (monazite and xenotime). Volkovich et al. showed that it was possible to form pure $REPO_4$ phases (Ln = La, Ce, Pr, Nd, Sm, Eu, Gd, Tb, and Dy) in LiCl–KCl and NaCl–KCl eutectics by adding lithium orthophosphate (Li_3PO_4) or sodium orthophosphate (Na_3PO_4) at 550 and 750 °C, respectively [10–12]. The same authors also reported that only a large excess of A_3PO_4 (A = Na and Li) compared with cerium chloride (PO_4^{3-}:Ce^{3+} molar ratio ≈ 5) allowed a $CeCl_3 \rightarrow CePO_4$ conversion factor of between 80% and 99%. This behavior was generalized to all the REE.

The work described here is part of the overall strategy for selectively and successively precipitating the different fission product families. The results discussed below concern only the preparation of rare earth phosphates ($REPO_4$) in molten LiCl–KCl eutectic (58.5–41.5 mol%) at 500 °C. The originality of this study lies in the use of ammonium dihydrogenphosphate ($NH_4H_2PO_4$, hereafter abbreviated ADP) as a phosphorus precursor to avoid modifying the mixture composition – unlike other precursors such as A_3PO_4 – by eliminating the chlorine bound to the rare earth elements as volatile gaseous species. As a starting point, this study will only consider separate rare earths even if, for the industrial operation, the molten salts would contain a mixture of numerous of these elements. Such a more complicated situation will be considered in a future work.

2. Experimental method

2.1. Experimental synthesis in molten chlorides

All the experiments were carried out using the experimental setup shown schematically in Fig. 3. It comprises a quartz reactor inside a Pekly vertical tube furnace (inside diameter, 75 mm).

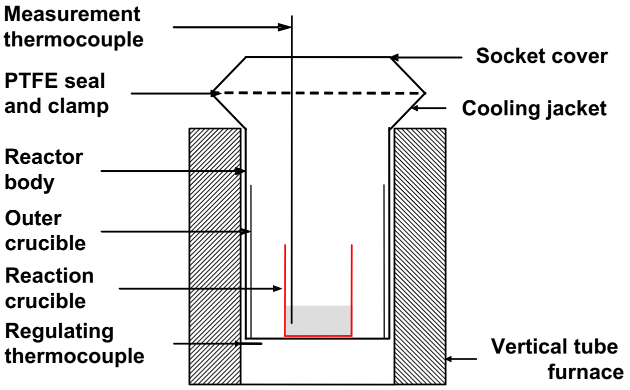

Fig. 3. Schematic representation of the experimental device used to synthesize lanthanide phosphates in molten LiCl–KCl.

Temperature control was provided by a power supply unit driven by a Eurotherm 2048 temperature regulator. The reactor with an overall height of 330 mm consisted of two separate units: a socket-type cover and a reactor body with a water-cooling jacket. Leak-tightness between the two reactor components is ensured by a PTFE-coated seal and a clamp. The lower portion of the reactor body accommodates an alumina reaction crucible (OD 30 mm, ID 25 mm and 40 mm high) and quartz outer crucible (OD 65 mm, ID 58 mm and 110 mm high). The gaseous reaction products are neutralized on exiting the reactor by bubbling in a 2 M. potassium hydroxide solution. The bath temperature is controlled by a thermocouple inside a quartz tube extending directly into the melt.

2.2. Preparation of the reaction mixture

All the experiments were carried out using the LiCl–KCl eutectic mixture as the solvent (58.5 mol% LiCl, melting point 353 C). A characteristic experiment was performed by mixing 9 g of LiCl–KCl eutectic (anhydrous LiCl 99% and KCl, xH$_2$O 99.99% previously heated to 250 °C overnight, Aldrich) and 1 g of anhydrous rare earth chloride (>99.9%, Aldrich). The phosphorus precursor (99%, Aldrich) was added to the mixture in stoichiometric quantity (P:RE molar ratio = 1). After homogenizing by manual grinding in an agate mortar the mixture was placed in the alumina crucible. All these operations were carried out in a glove box under anhydrous conditions in argon atmosphere. The alumina crucible was then placed in the quartz reactor and heated in air to 500 °C at a heating rate of 5 °C min^{-1}. The target temperature was maintained for 5 h after which the heating was switched off and the mixture was allowed to cool to room temperature.

2.3. Sample treatment and characterization methods

After cooling and solidification the resulting salt blocks were subjected to one of two types of treatment. The first, systematically used in the literature for this type of investigation [6,7,10–12], consisted in dissolving the solvent in an aqueous solution. In this study, salt blocks of about 10 g were placed in 200 mL of deionized water at room temperature and stirred magnetically for 30 min. The resulting precipitate was filtered, rinsed in deionized water, and dried overnight at 120 °C. The dry powder recovered was qualitatively analyzed by X-ray diffraction (XRD).

It should be noted, however, that exposing the reaction product to an aqueous medium is liable to modify it – especially by dissolving possible secondary phases formed in the molten bath. It is the reason why a second procedure was used in order to characterize the mixture after the reaction: the salt blocks solidified in the quartz reactor were recovered at 150 °C and placed directly in an anhydrous glove box to minimize hydration. The elapsed time between removal of the reaction crucible from the furnace and transfer of the salt block into the glove box airlock was less than 1 min. Before characterization the blocks were simply ground manually in an agate mortar to obtain a powder. At this stage all the constituents of the initial reaction mixture were present together with all the phases formed in the molten salt.

2.3.1. Powder X-ray diffraction (XRD)

The phases obtained were characterized at room temperature (20 °C) in Bragg–Brentano geometry using a Brüker D8 diffractometer with a copper anticathode ($\lambda = 1.540598$ Å) and a monochromator. Rietveld pattern fitting [13] was performed using Jana 2006 software [14].

2.3.2. Solid-state NMR

The samples not treated in aqueous media were characterized by solid-state ^{31}P NMR experiments. The ^{31}P magic angle spinning (MAS) NMR spectra were obtained with a Bruker AVANCE 400 spectrometer operating at 161.99 MHz for ^{31}P. The powder samples were packed into 4 mm zirconia rotors and spun at 14 kHz at the magic angle (MAS). Single pulse spectra were recorded by using 10° pulses with an optimized delay time of 5 s. Chemical shifts are reported relative to 85% H$_3$PO$_4$. All NMR spectra were modeled using the Dmfit program [15].

3. Results and discussion

3.1. Nature of phases formed by individual lanthanides: characterization after aqueous treatment

The reactivity of various rare earth chlorides taken individually was estimated in LiCl–KCl eutectic in contact with ADP. For all these experiments the solvent was loaded with 10 wt% of the rare earth chloride. The composition of the test mixtures and the experimental conditions are summarized in Table 2.

For the test compositions, dissolution of the salt blocks resulted in particles in suspension in the water. All the particles were white except for praseodymium and neodymium, which gave green and violet particles, respectively. XRD analysis with Rietveld refinement by fundamental approach is shown in Figs. 4 and 5 for lanthanum and lutetium systems respectively. For the lanthanum system (Ln-01), results of the refinement are gathered in Table 3 and Fig. 4. We can clearly see the formation of pure LaPO$_4$ with monazite structure (space group $P2_1/n$). Profiles and intensities are in good agreement between experimental and calculated patterns. In agreement with published findings [16] the lightest rare earth elements (La Ce, Pr, and Nd) formed phosphates with monazite structure. For the lutetium system (Ln-05), results of the refinement are gathered in Table 4 and Fig. 5. Oxidation numbers calculated and electronic density residues are in good agreement with the xenotime structure formation (space group $I4_1/amd$).

Moreover, the conversion of rare earth chlorides to rare earth phosphates was estimated more quantitatively using the conversion factor η (Table 5) defined as $\eta = m_{\mathrm{exp}}/m_{\mathrm{th}}$, where m_{exp} and m_{th} are the experimental and theoretical REPO$_4$ phosphate mass values, assuming complete conversion.

Note that for a P:RE molar ratio of 1, η ranged from 96% (Nd, Lu) to 98% (La, Ce and Pr). This difference in behavior with regard to the conversion factor according to the type of rare earth element could be attributable to a difference in the stability of the complexes formed within the liquid, although this hypothesis must be verified. Nevertheless, these η values are similar to those obtained by Volkovich et al. with conversion factor ranging from 90% to 99% depending on the nature of the RE [10]. Moreover, using ammonium dihydrogenphosphate as a phosphorus precursor ensures quantitative conversion of RECl$_3$ to REPO$_4$ simply by stoichiometric addition, and constitutes a significant difference with the

Table 2
Composition of reaction mixtures tested for precipitation of individual RE elements

Reference	Composition of test mixtures mol%				Ln	Experimental conditions
	LiCl	KCl	RECl$_3$	Ln:P molar ratio		
Ln-01	57	40.5	2.5	1	La	Heating rate, 5 °C min^{-1}
Ln-02	57	40.5	2.5	1	Ce	Target temperature, 500 °C
Ln-03	57.1	40.5	2.4	1	Pr	Residence time, 5 h
Ln-04	57.1	40.5	2.4	1	Nd	Cooling rate, not controlled
Ln-05	57.2	40.6	2.2	1	Lu	Atmosphere, air

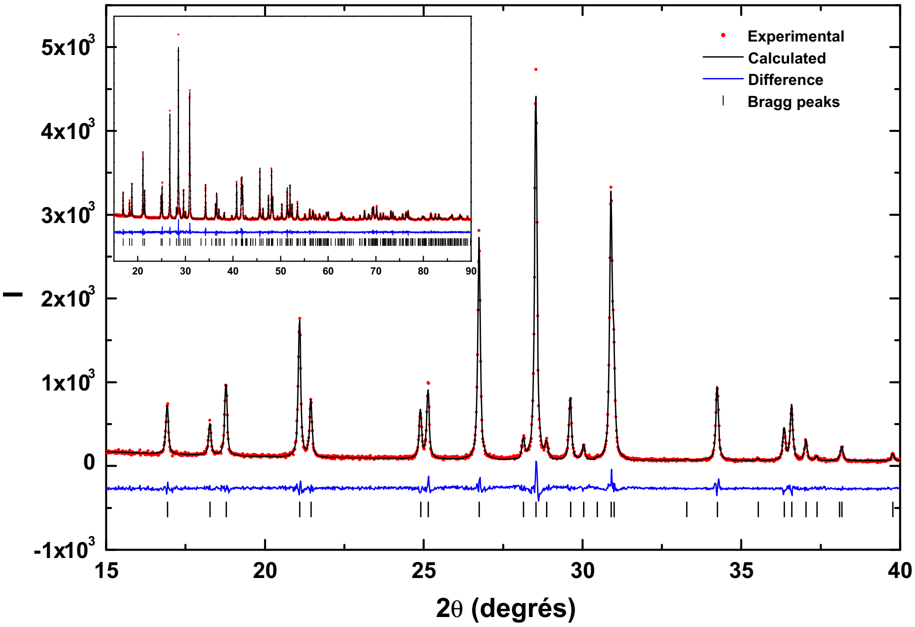

Fig. 4. Refinement (JANA) obtained after aqueous treatment of mixtures $(LiCl–KCl)_e + NH_4H_2PO_4 + LaCl_3$ (La:P = 1) reacted at 500 °C for 5 h in air.

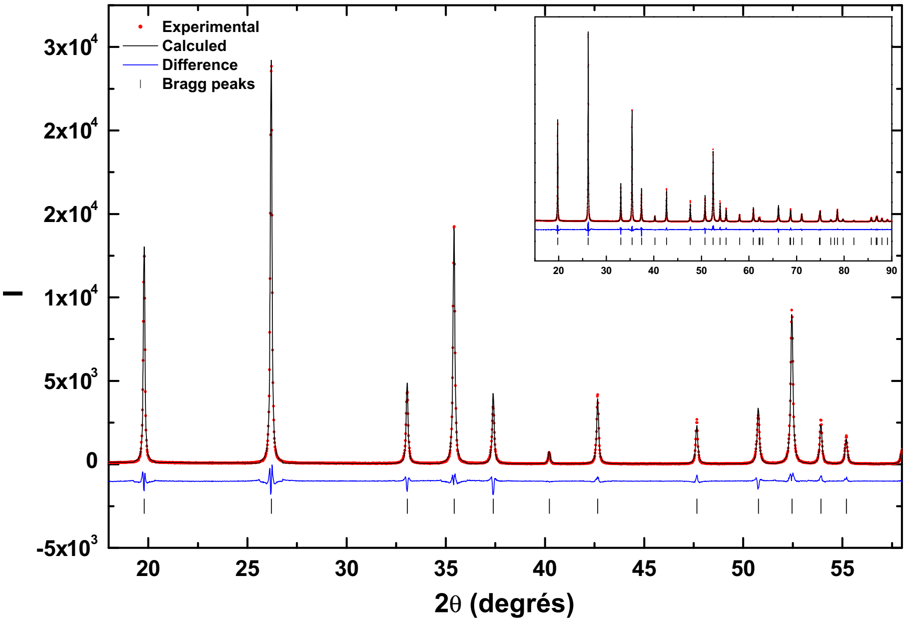

Fig. 5. Refinement (JANA) obtained after aqueous treatment of mixture $(LiCl–KCl)_e + NH_4H_2PO_4 + LuCl_3$ (Lu:P = 1) reacted at 500 °C for 5 h in air.

behavior of alkali orthophosphates, which must be added in excess (P:RE = 5) to obtain comparable conversion factors.

During all the experiments a white deposit was observed on all the cold surfaces of the reactor (Fig. 6(a)). The deposit was recovered and analyzed by XRD, revealing pure ammonium chloride (Fig. 6(b)).

Ammonium chloride was observed to form during all the experiments with the rare earth elements. The initial results demonstrate quantitative precipitation of rare earth phosphates in molten $(LiCl–KCl)_e$ from the corresponding chlorides ($RECl_3$) and $NH_4H_2PO_4$. The reaction involved can be described by the following general relation:

$$RECl_3 + NH_4H_2PO_4 \overset{\Delta}{\rightarrow} REPO_4 + NH_4Cl + 2HCl$$

Nevertheless, some doubt remains as to whether or not treatment in aqueous media after the reaction can modify the nature of the phases obtained after cooling. ^{31}P NMR characterization was, therefore, performed on all the salt blocks without aqueous treatment.

3.2. Characterization of mixtures without aqueous treatment

When the salt blocks were removed from the reaction crucible (without aqueous treatment), two distinct material zones were observed, suggesting that demixing had occurred between the flux and the rare earth phosphate formed in situ. The zone with the larger volume was always white – regardless of the composition of the test mixture – and was found at the top of the salt block.

Table 3
Refinement of the $LaPO_4$ compound obtained after reaction at 500 °C for 5 h in air for $\{(LiCl–KCl)_e + NH_4H_2PO_4 + LaCl_3$ (La:P = 1)} system

Phase	Space group		Cell parameters (Å)			Volume (Å^3) 306.930
Monoclinic	*P21/n*		*a*	*b*	*c*	
			6.84444 (7)	7.07802 (7)	6.51115 (6)	
			γ = 103.3339 (7)			
Atom	Site	Site occupancy	*x*	*y*	*z*	Uiso
La1	4e	1	0.28253 (18)	0.16005 (18)	0.1008 (2)	0.0199 (4)[a]
P1	4e	1	0.3024 (7)	0.1644 (7)	0.6090 (8)	0.0198 (12)
O1	4e	1	0.2473 (14)	0.0107 (13)	0.4407 (15)	0.0096 (15)
O2	4e	1	0.3805 (11)	0.3299 (14)	0.4995 (14)	0.0096 (15)
O3	4e	1	0.4684 (13)	0.1058 (11)	0.7933 (13)	0.0096 (15)
O4	4e	1	0.1306 (14)	0.2082 (12)	0.7034 (15)	0.0096 (15)

[a] U11 0.0218 (7); U22 0.0167 (7); U33 0.0209 (7); U12 0.0014 (11); U13 0.0041 (5) and U23 −0.0035 (12).

Table 4
Refinement of the $LuPO_4$ compound obtained after reaction at 500 °C for 5 h in air for $\{(LiCl–KCl)_e + NH_4H_2PO_4 + LuCl_3$ (Lu:P = 1)} system

Phase	Space group		Cell parameters (Å)			Volume (Å^3)
Tetragona l	*I4$_1$/amd*		*a*	*b*	*c*	275.208 (4)
			6.79605 (6)	6.79605	5.95865 (6)	
Atom	Site	Site occupancy	*x*	*y*	*z*	Uiso
Lu1	4a	0.906 (6)	0	0.75	0.125	0.0083 (3)[a]
P1	4b	1	0	0.25	0.375	0.0124 (15)
O1	16h	1	0	0.4273 (6)	0.2153 (6)	0.0214 (17)

[a] U11 0.0100(4); U22 0.0100(4); U33 0.0049(7); U12 0; U13 0 and U23 0.

Table 5
Conversion factors obtained experimentally for precipitation of individual rare earth elements by adding $NH_4H_2PO_4$ to a eutectic mixture of LiCl–KCl + $RECl_3$ with P:RE molar ratio of 1

Solid phase composition (XRD)/structure		η (%)
$LaPO_4$	Monazite	98
$CePO_4$		98
$PrPO_4$		98
$NdPO_4$		96
$LuPO_4$	Xenotime	95

The lower part of the block can be white (experiments with La, Ce, and Dy), green (Pr) or violet (Nd, Fig. 7).

^{31}P MAS NMR characterizations were therefore carried out on complete mixtures (LiCl–KCl + $RECl_3$ + $NH_4H_2PO_4$). Only the results obtained with the lanthanum reaction mixture are shown, however, because of the paramagnetism of the other rare earth elements studied. The ^{31}P MAS spectrum of the lanthanum mixture before heating (Fig. 8) was characterized by a peak modeled by a single Lorentzian line with a chemical shift δ_{iso} ^{31}P of +1.1 ppm. This value is consistent with published data for $NH_4H_2PO_4$ (0.9 and 1 ppm) [17,18]. After the reaction, the ^{31}P MAS NMR spectrum for the mixture was still characterized by a single peak (Fig. 8) with an isotropic chemical shift of −4.3 ppm, characteristic of lanthanum monazite [19]. Characterization without post-reaction treatment not only shows that the formation of lanthanum phosphate is not the result of aqueous treatment, but also that a pure phase was formed. Moreover, the fact that no other peak was visible by ^{31}P MAS NMR suggests that there is only a single phosphorus environment. The conversion of lanthanum chloride to lanthanum phosphate was therefore near 100%, in good agreement with η calculated by comparing the theoretical and experimental $LaPO_4$ mass values. As the other lanthanides tested are paramagnetic, their

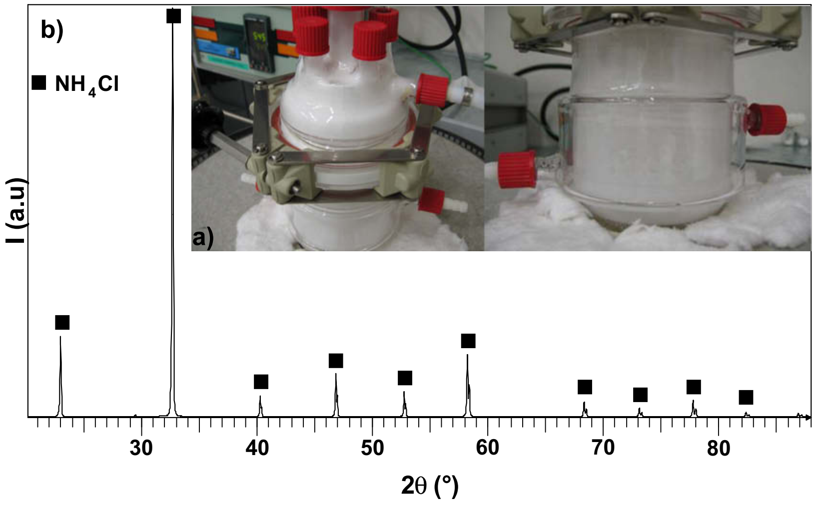

Fig. 6. (a) Appearance of cold reactor surfaces after reaction (500 °C, 5 h in air) of a mixture of LiCl–KCl + $RECl_3$ + $NH_4H_2PO_4$ and (b) XRD analysis of deposit.

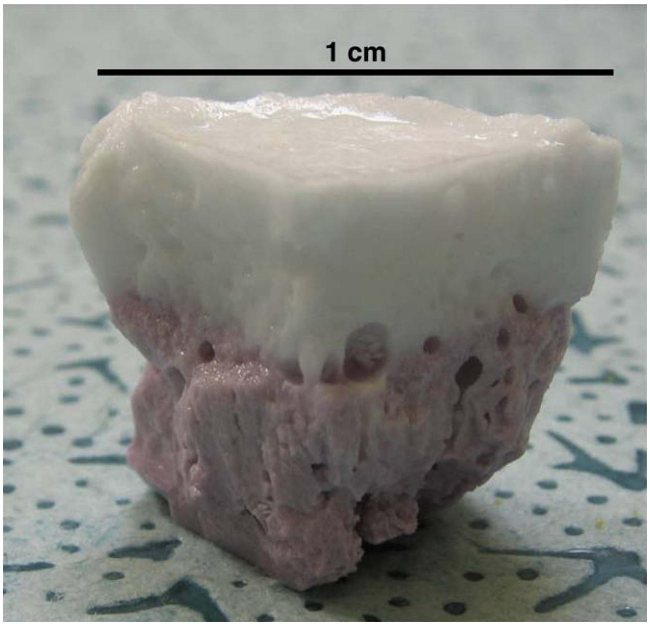

Fig. 7. Salt block removed from the crucible after reaction (500 °C for 5 h in air) of a mixture of $(LiCl–KCl)_e + NdCl_3 + NH_4H_2PO_4$, P:Nd = 1.

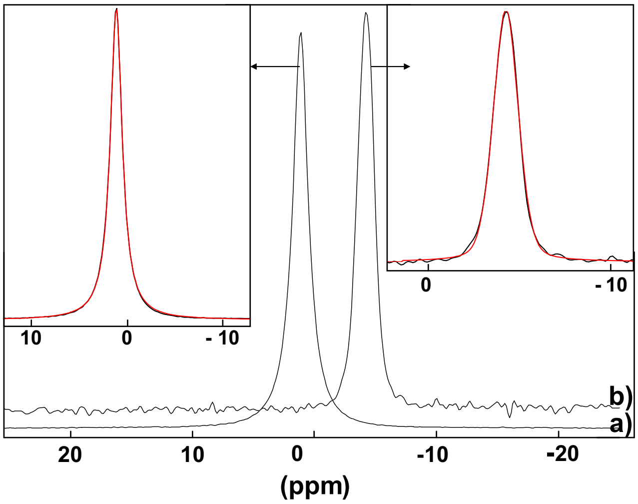

Fig. 8. Experimental (a and b) and modeled (insets) ^{31}P MAS NMR spectra of complete reaction mixture $LiCl–KCl + LaCl_3 + NH_4H_2PO_4$ (P:La = 1). Left; before reaction, right; after reaction in air at 500 °C for 5 h without subsequent aqueous treatment.

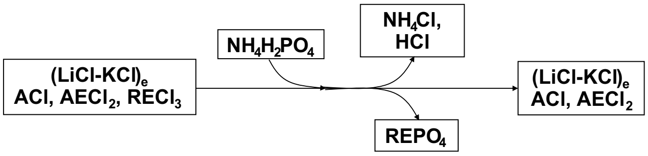

Fig. 9. Schematic representation of selective precipitation of rare earth elements as rare earth phosphates $REPO_4$. Method based on equimolar P:RE addition and on simultaneous elimination of the chlorine bound to the rare earth elements by the formation of volatile gaseous species.

MAS NMR spectra were of lower resolution and the purity of the resulting phosphates cannot be affirmed with certainty. Nevertheless, the conversion factors η were near that of lanthanum, suggesting that only rare earth phosphates $REPO_4$ are formed in a molten $(LiCl–KCl)_e$ medium.

4. Conclusion

The originality of this study lies in the use of $NH_4H_2PO_4$ as a phosphorus precursor in molten LiCl–KCl eutectic for synthesizing rare earth phosphates ($REPO_4$) with monazite or xenotime structures. Unlike the use of alkali orthophosphates, this method provides similar conversion factors with the simple addition of stoichiometric phosphorus (P:RE = 1) and does not require excess phosphate (P:RE = 5). This prevents the formation of a secondary Li_3PO_4 phase. Moreover, ammonium dihydrogenphosphate also allows chlorine bound to rare earth elements to be eliminated as NH_4Cl. The formation of HCl is strongly suspected. Adding ammonium dihydrogenphosphate to a molten LiCl–KCl medium containing rare earth chlorides thus allows quantitative precipitation of rare earth phosphates without affecting the nature and quantity of the solvent at the end of the experiment. From the standpoint of managing chlorinated salts loaded with fission products, this method could be used as the first step in processing the waste stream (Fig. 9), resulting in a partially purified mixture containing only alkali and alkaline earth chlorides.

However, ammonium dihydrogenphosphate is known to be thermally unstable [20–22]. Although the decomposition mechanisms have never been clearly identified, most studies have shown that the pure compound begins to decompose at about 170–200 °C. Moreover, ammonium dihydrogenphosphate decomposition can be affected by the chemical nature of the reaction medium. In order to understand the formation of rare earth phosphates in a molten chloride medium, additional studies are therefore in progress to identify the intermediate reaction products involved in the formation of rare earth phosphates.

References

[1] US-DOE/GIF, December 2002. A Technology Roadmap for Generation IV Nuclear Energy Systems, GIF-002-00. Available at: <http://www.gen-4.org/>.
[2] G.R. Choppin, M.Kh. Khankhasayev (Eds.), Proceedings of the NATO Advanced Study Institute on Chemical Separation Technologies and Related Methods of Nuclear Waste Management: Applications, Problem and Research Needs, Dubna, Russia, 18–28 May 1998.
[3] S.K. Fong, I.W. Donald, B.L. Metcalfe, J. Alloys Compd. 444&445 (2007) 424.
[4] DOE, Electrometallurgical Techniques for DOE Spent Fuel Treatment, Final Report, 2000. Available at: <http://www.nap.edu/catalog/9883.html>.
[5] I.W. Donald, B.L. Metcalfe, S.K. Fong, L.A. Gerrard, D.M. Strachan, R.D. Scheele, J. Nucl. Mater. 361 (2007) 78.
[6] Y.-J. Cho, H.-C. Yang, H.-C. Eun, E.-H. Kim, J.-H. Kim, J. Ind. Eng. Chem. 11 (2005) 707.
[7] Y.-J. Cho, H.-C. Yang, H.-C. Eun, E.-H. Kim, I.-T. Kim, J. Nucl. Sci. Technol. 43 (2006) 1280.
[8] S.V. Ushakov, K.B. Helean, A. Navrotsky, J. Mater. Res. 16 (2001) 2623.
[9] L.A. Boatner, Rev. Mineral. Geochem. 48 (2002) 87.
[10] V.A. Volkovich, T.R. Griffiths, R.C. Thied, Phys. Chem. Chem. Phys. 5 (2003) 3053.
[11] V.A. Volkovich, T.R. Griffiths, R.C. Thied, J. Nucl. Mater. 323 (2003) 49.
[12] T.R. Griffiths, V.A. Volkovich, S.M. Yakimov, I. May, C.A. Sharrad, J.M. Charnock, J. Alloys Compd. 418 (2006) 116.
[13] H.M. Rietveld, J. Appl. Cryst. 2 (1969) 65.
[14] V. Petricek, M. Dusek, L. Palatinus, Jana2006. The crystallographic computing system, Institute of Physics, Praha, Czech Republic, 2006.
[15] D. Massiot, F. Fayon, M. Capron, I. King, S. Le Calve, B. Alonso, J.O. Durand, B. Bujoli, Z. Gan, G. Hoatson, Magn. Reson. Chem. 40 (2002) 70.
[16] Y. Ni, J.M. Hughes, Am. Mineral. 80 (1995) 21.
[17] K. Eichele, R.E. Wasylishen, J. Phys. Chem. 98 (1994) 3108.
[18] G.L. Turner, K.A. Smith, R.J. Kirkpatrick, E. Oldfield, J. Magn. Reson. 70 (1986) 408.
[19] D. Bregiroux, F. Audubert, T. Charpentier, D. Sakellariou, D. Bernache-Assollant, Solid State Sci. 9 (2007) 432.
[20] E. Torijano, R.A. Vargas, J.E. Diosa, B.-E. Mellander, Phys. Status Solidi B 220 (2000) 659.
[21] A. Abdel-Kader, A.A. Ammar, S.I. Saleh, Thermochim. Acta 176 (1991) 293.
[22] M. Maciejewski, R. Rudnicki, Thermochim. Acta 113 (1987) 305.